Selective uveal melanoma inhibition with calcium channel blockade

MICHAEL SHAUGHNESSY[1,2*], GRACE LAMURAGLIA[1*], NIKOLAI KLEBANOV[1,2], ZHENYU JI[1], ANPUCHCHELVI RAJADURAI[1], RAJ KUMAR[1], KEITH FLAHERTY[3] and HENSIN TSAO[1,4]

[1]Wellman Center for Photomedicine, Massachusetts General Hospital, Harvard Medical School, Boston, MA 02114-2605; [2]Tufts University School of Medicine, Boston, MA 02111; [3]Department of Medicine, Division of Medical Oncology, Massachusetts General Hospital Cancer Center, Center for Melanoma, Harvard Medical School, Boston, MA 02114-2605; [4]Department of Dermatology, Massachusetts General Hospital, Harvard Medical School, Boston, MA 02114-2605, USA

Received June 19, 2019; Accepted August 6, 2019

DOI: 10.3892/ijo.2019.4873

Abstract. Uveal malignant melanoma (UMM), the most common primary adult intraocular tumor with a marked metastatic potential, is genetically unique and has unfortunately had few treatment breakthroughs. In this study, we subjected a UMM cell line to high-throughput library screening with 1,018 FDA-approved compounds to identify potential UMM-selective cytotoxic agents. Amlodipine, a dihydropyridine calcium channel blocker (CCB), ranked no. 2 and no. 8 of the most cytotoxic compounds. Thus, we further characterized the differential effects of calcium blockade on UMM and cutaneous malignant melanoma (CMM) lines *in vitro* using growth inhibition, cell cycle progression, apoptosis and senescence assays. Amlodipine had a significantly higher growth inhibitory potency in UMM (IC_{50}=13.1 μM) than CMM (IC_{50}=15.9 μM, P<0.05) lines. In 3D spherical cell culture, amlodipine treatment significantly impaired tissue volume growth in two UMM lines, but exerted no significant effects among all 3 CMM lines tested. Treatment with 10 and 20 μM amlodipine induced a significant impairment of cell cycle progression and the apoptosis of UMM lines, implicating both of these processes as mediators of the observed growth inhibition in UMM compared to CMM. On the whole, the findings of this study suggest that calcium channel blockade is a potentially effective strategy for selective uveal melanoma targeting.

Correspondence to: Professor Hensin Tsao, Wellman Center for Photomedicine, Massachusetts General Hospital, Harvard Medical School, 50 Blossom Street, EDR 221, Boston, MA 02114-2605, USA
E-mail: HTSAO@mgh.harvard.edu

*Co-first authorship

Key words: uveal melanoma, melanoma, amlodipine, calcium homeostasis, drug screening, ophthalmology

Introduction

Uveal malignant melanoma (UMM) is a rare cancer of the melanocytes of the iris, ciliary body, and choroid eye structures (1). While UMM accounts for only 5% of all melanoma cases and has a yearly incidence of just 5 cases per one million in the United States (2,3), it is the most common intraocular malignancy affecting adults and the most commonly occurring non-cutaneous form of melanoma (4,5). Despite effective primary tumor management, one half of UMM cases progress to metastatic disease, after which survival is usually <1 year (6,7).

The successful use of targeted gene therapies, such as BRAF and MEK inhibitors in cutaneous malignant melanoma (CMM) has not translated to UMM. This is due in part to the genetically distinct mutational landscape of UMM, which lacks the driver mutations common to CMM, and to the rarity of the disease, which limits patient availability for clinical trials (8). Trials with traditional chemotherapeutic agents, such as dacarbazine and with novel immunotherapies, such as checkpoint inhibitors have both failed to lead to a reduction in the mortality rate (9-11), and there is currently no FDA-approved therapy available for UMM (12).

In this study, we discuss our use of a discovery-based approach to identify already-existing therapies that have potential activity against uveal melanoma. Using high-throughput library screening with a large panel of FDA-approved drugs on a UMM cell line, we ranked the activity of each drug against UMM, and then further characterized the discovered top-ranking calcium channel blocker class of medications using *in vitro* studies. Our findings suggest that the calcium signaling pathway may mediate the downstream signaling of mutant *GNAQ*, a common uveal melanoma driver mutation. Calcium channel blockade may thus be a potential strategy for the treatment of uveal melanoma.

Materials and methods

Melanoma cell lines. We have adopted stringent criteria for establishing the identity of the cell lines used in this study. New lines are purchased directly from trusted repositories

(e.g., ATCC), while legacy cell lines (e.g., those cell lines which are gifts from collaborators) are stratified into 3 levels of confidence after sequencing. 'CONFIRMED' cell lines are either new lines from ATCC or those which have demonstrated an unequivocal match between our designation and the STR database after STR genotyping. For those with 'no hits' in the STR database, we performed a manual search of key melanoma mutations [e.g., BRAF(V600E), NRAS(Q61), etc.] reported for each line in either the Catalogue Of Somatic Mutations In Cancer (COSMIC), the Cancer Cell Lines Encyclopedia (CCLE), or in individual publications in the literature. We subsequently compared Sanger or whole exome sequence information generated in our laboratory for these lines, and if there is a direct match between our sequence information and the public domain data, these cell lines are designated as 'CONSISTENT'. For cell lines without public domain information, we analyzed the levels of MITF (M-isoform) to determine whether the cells are compatible with melanocytic cells. Those that express significant M-isoform MITF are designated as 'COMPATIBLE'.

When selecting cell lines for experimentation, the order of preferential selection is 'CONFIRMED' > 'CONSISTENT' > 'COMPATIBLE'. Furthermore, all cell lines have been tested for common pathogens, such as mycoplasma, and are pathogen-free. The following are accession numbers for cell lines from Cellosaurus (web.expasy.org/cgi-bin/cellosaurus/search): MP41 (CVCL_4D12), Mel-270 (CVCL_C302), Mel-202 (CVCL_C301), OMM2.3 (CVCL_C306), CHL-1 (CVCL_1122), MeWo (CVCL_0445), SK-MEL-2 (CVCL_0069), SK-MEL-119 (CVCL_6077), Mel JuSo (CVCL_1403), IPC-298 (CVCL_1307), UACC-903 (CVCL_4052), SK-MEL-28 (CVCL_0526) and A375 (CVCL_0132).

High-throughput candidate drug screening. To initially identify UMM-active compounds, the UMM cell line, OMM2.3, was subjected to viability screening using an FDA-approved Drug Library (Selleckchem) that included 1,018 drugs (Table SI). Cells were seeded at 2,000 cells/well using an automated plate filler in a 384-well plate and incubated for 24 h at 37˚C. Subsequently, a 3 μM concentration of each drug was added to the plate via pin-transfer and the plates were incubated for an additional 72 h at 37˚C. Drug efficacy was measured via a proliferation ratio using CellTiter-Glo® Luminescence assay (Promega) and an EnVision plate reader (PerkinElmer).

Two-dimensional cell viability. Based on the results of this initial drug screen, 4 UMM (MP41, Mel-270, Mel-202 and OMM2.3) and 10 CMM (CHL-1, MeWo, SK-MEL-2, SK-MEL-119, Mel JuSo, IPC-298, UACC-903, SK-MEL-28, MGH-CH-1 and A375) cell lines were selected for additional drug screening analysis with the dihydropyridine calcium channel blocker (CCB), amlodipine (Selleck Chemicals), and the non-dihydropyridine CCBs, verapamil and diltiazem (Sigma-Aldrich). The cells were seeded at 2,000 cells/well in 96-well plates, incubated at 37˚C for 24 h, and subjected to 9 doses of each drug in triplicate. Cell viability was measured after 72 h of incubation at 37˚C in the presence of drug using CellTiter-Glo® Luminescence assay (Promega). An equivalent volume of DMSO was used as a control, and the results were normalized to this control value. IC_{50} values were calculated using GraphPad Prism software (Version 7) and compared between the UMM and CMM lines using two-sided t-tests. Intracellular calcium depletion after 48 h of treatment with 0, 2, 4 and 8 μM amlodipine was additionally visualized using 1 μM calcium-sensitive Rhod 2 fluorescent dye (Thermo Fisher Scientific) on one UMM line (OMM2.3) and one CMM line (A375).

All CMM lines were cultured in Dulbecco's modification of Eagle's medium (DMEM; Thermo Fisher Scientific) with 10% fetal bovine serum (FBS; Atlanta Biologicals) and 1% penicillin/streptomycin (Thermo Fisher Scientific). UMM lines were cultured in RPMI-1640 with 10% FBS, 1% each of HEPES, L-glutamine, penicillin/streptomycin, and 0.1% of β-mercaptoethanol (all from Thermo Fisher Scientific).

Three-dimensional (3D) spheroid model. We then performed drug screening analyses on a smaller cohort of melanoma cell lines in a 3D culture system to evaluate the ability of the drug to penetrate a tumor-like spheroid. For spheroid generation in 3D culture, 100 μl of Matrigel® were added to 96-well plates followed by incubation at 37˚C for 1 h to allow for matrix solidification. Cell lines suspended in 70 μl of their respective growth media were then seeded on top of the matrix base at an empirically-determined density to allow for proper growth over the experimental duration (A375 cells, 800 cells/well; CHL-1 cells, 1,000 cells/well; IPC-298 cells, 2,000 cells/well; MP41 cells, 2,500 cells/well; OMM2.3 cells, 2,500 cells/well). Following an additional incubation at 37˚C for 30 min, a 10 μl mixture of Matrigel® and DMEM (at a ratio of 1:10, respectively) was carefully transferred to each well and allowed to settle to the bottom of the cell culture medium. Thus, the cell layer was secured in place between 2 layers of Matrigel® extracellular matrix.

The cells were cultured for 11 days to allow for spheroid formation, after which time a 20 μM concentration of amlodipine was added on day 0. Following a 48-h incubation at 37˚C in the presence of drug or the DMSO control, the diameter of randomly-sampled spheroids in each colony was measured on day 2 using light microscopy (Zeiss Axiovert 100 TV) and ImageJ software. Mean spheroid diameters for each colony were calculated from these measurements and normalized to the mean diameter of the corresponding cell line's colonies on day 0. The normalized mean diameters on day 2 were compared between conditions using two-sided t-tests.

Cell cycle, apoptosis and senescence. To characterize the mechanism responsible for the observed inhibitory effects of calcium channel blockade, we performed several functional assays on UMM and CMM cell lines. Cell cycle analysis was first performed using propidium iodide (PI) staining. The cell lines were plated on 6-well plates at 50% confluence and cultured for 24 h. They were then treated with 5, 10 or 20 μM of amlodipine and incubated at 37˚C for an additional 24 h. The cells were then trypsinized, centrifuged at room temperature (1,500 rpm, 5 min), and washed with PBS. Following re-suspension in 100 μl of 1X PBS, 250 μl of 70% cold ethanol was added drop-wise while vortexing. The samples were frozen at -20˚C overnight for fixation. The following day, the cells were thawed, and the ethanol was removed. The cells were then washed with 1X PBS and resuspended in 0.5 ml

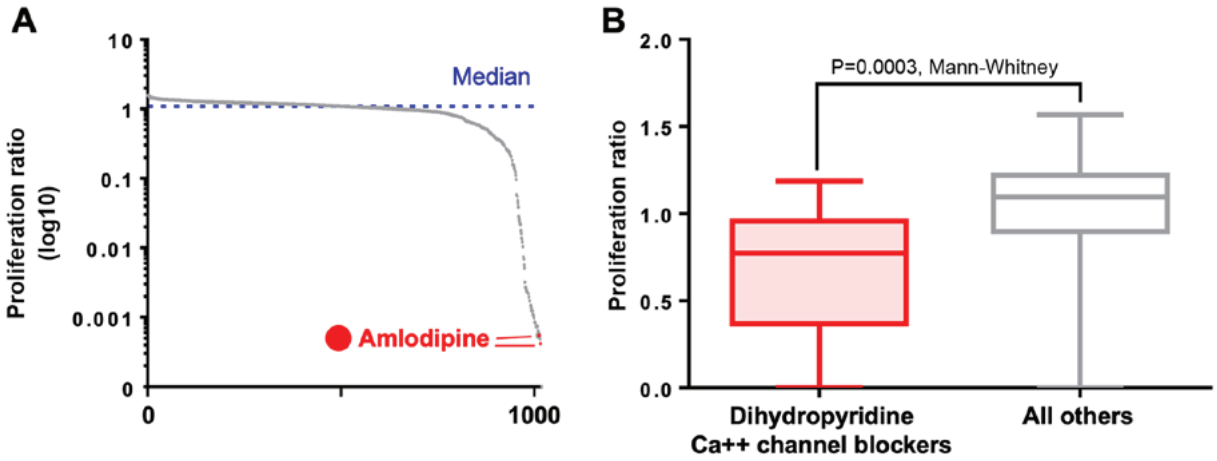

Figure 1. High-throughput drug screening results. (A) Plot of the proliferation ratio in all 1,018 screened compounds in high-throughput drug screening analysis. (B) Comparison of the proliferation ratio of the dihydropyridine class vs. all other screened compounds in high-throughput drug screening analysis.

PI staining solution [1 ml of PI (100 μg/ml), 80 μl of RNAse (100 μg/ml), and 20 μl of NP-40 (0.1%); Molecular Probes] prior to incubation at room temperature in the dark for 30 min. All analyses were performed on FACSCalibur Flow Cytometer (BD Biosciences).

After observing significant growth inhibition in our cell viability analyses, we hypothesized that amlodipine may be initiating its effects on cell growth through the induction of apoptosis. We used Annexin V expression as an early apoptotic marker. An Alexa Fluor 488 Annexin V/PI staining kit was used following the manufacturer's protocol (Life Technologies; Thermo Fisher Scientific). Briefly, the cells were collected after 24 h of 5, 10 or 20 μM amlodipine treatment, washed twice with PBS, and stained with Alexa Fluor Annexin V for 20 min followed by PI for 1 min both at room temperature. Flow cytometry was performed on a BD FACSAria (BD Biosciences), and all data were analyzed using FlowJo 10.0.8 software.

To detect for the association of a senescent-associated effect of amlodipine treatment, 2 UMM (MP41 and OMM2.3) and 2 CMM (A375, CHL-1 and IPC-298) cell lines were plated on a 12-well plate and cultured for 24 h. The cells were then treated with 3 different concentrations of (2, 4 and 8 μM) of amlodipine and incubated at 37˚C for an additional 48 h. The medium was then removed, and the cells were washed with 1X PBS followed by the addition of 0.5 ml of fixing solution for 15 min. The plate was again washed with 1X PBS prior to the addition of 0.5 ml of staining solution mix detection kit (470 μl staining solution, 5 μl staining supplement, 25 μl of 20 mg/ml SA-β-gal in DMF; BioVision). The cells were incubated overnight at 37˚C and senescence was visualized at 24 h using light microscopy (Zeiss Axiovert 100 TV).

Western blot analysis. Western blot analysis was also preformed to validate the apoptotic effects. Uveal lines (MP41 and OMM2.3) were grown on 60 mm plates, treated with either 10 μM of amlodipine or an equivalent volume of DMSO for the controls, and incubated at 37˚C for 24 h. Protein extraction was then performed using RIPA buffer (50 mM Tris-HCl, 150 mM NaCl, 1% NP-40, 0.5% sodium deoxycholate, and 0.1% SDS; Boston Bioproducts). A Lowry assay was performed to determine protein quantification, and sample concentrations were adjusted accordingly based on the standard curve produced. A total of 10 μg of each sample were loaded per well and run through a 4-12% SDS-PAGE gel prior to transfer to a nitrocellulose membrane (Bio-Rad Laboratories). Following incubation with 5% non-fat milk in TBST for 1 h at room temperature, the membrane was washed with TBST and probed with rabbit antibodies against cleaved PARP (cat. no. 9541s; Cell Signaling Technology) and mouse antibodies against GAPDH as a loading control (cat. no. ab8245; Abcam) at a 1:3,000 dilution for 16 h at room temperature. The blots were washed again with TBST and then incubated with a 1:5,000 dilution of horseradish peroxidase-conjugated anti-rabbit (cat. no. 7074s; Cell Signaling Technology) or anti-mouse antibodies (cat. no. 7076s; Cell Signaling Technology) for 16 h at 4˚C. The blots were washed again with TBST and developed with Clarity western ECL substrate (Bio-Rad Laboratories).

Statistical analysis. All viability and functional assays were performed in triplicate and with biological replicates of each class of melanoma cell lines (UMM and CMM) where appropriate. The Student's t-test was used to perform both comparisons of mean IC_{50} values following two-dimensional CCB treatment in CMM vs. UMM and comparisons of mean spheroid growth after three-dimensional CCB treatment in treated vs. control groups of each individual cell line. The comparison of apoptosis induction between treated and control groups was performed using one-way ANOVA and Dunnett's multiple comparisons test (with control group as reference). Significant differences for all tests were assumed at P-values <0.05. All statistical analyses were performed using GraphPad Prism 8 software.

Results

The initial library screening identified amlodipine as the no. 2 and no. 8 most active compound in UMM out of the 1,018 screened compounds (Fig. 1A and Table SI). The dihydropyridine CCB class as a whole had a significantly lower proliferation ratio than all other screened compounds

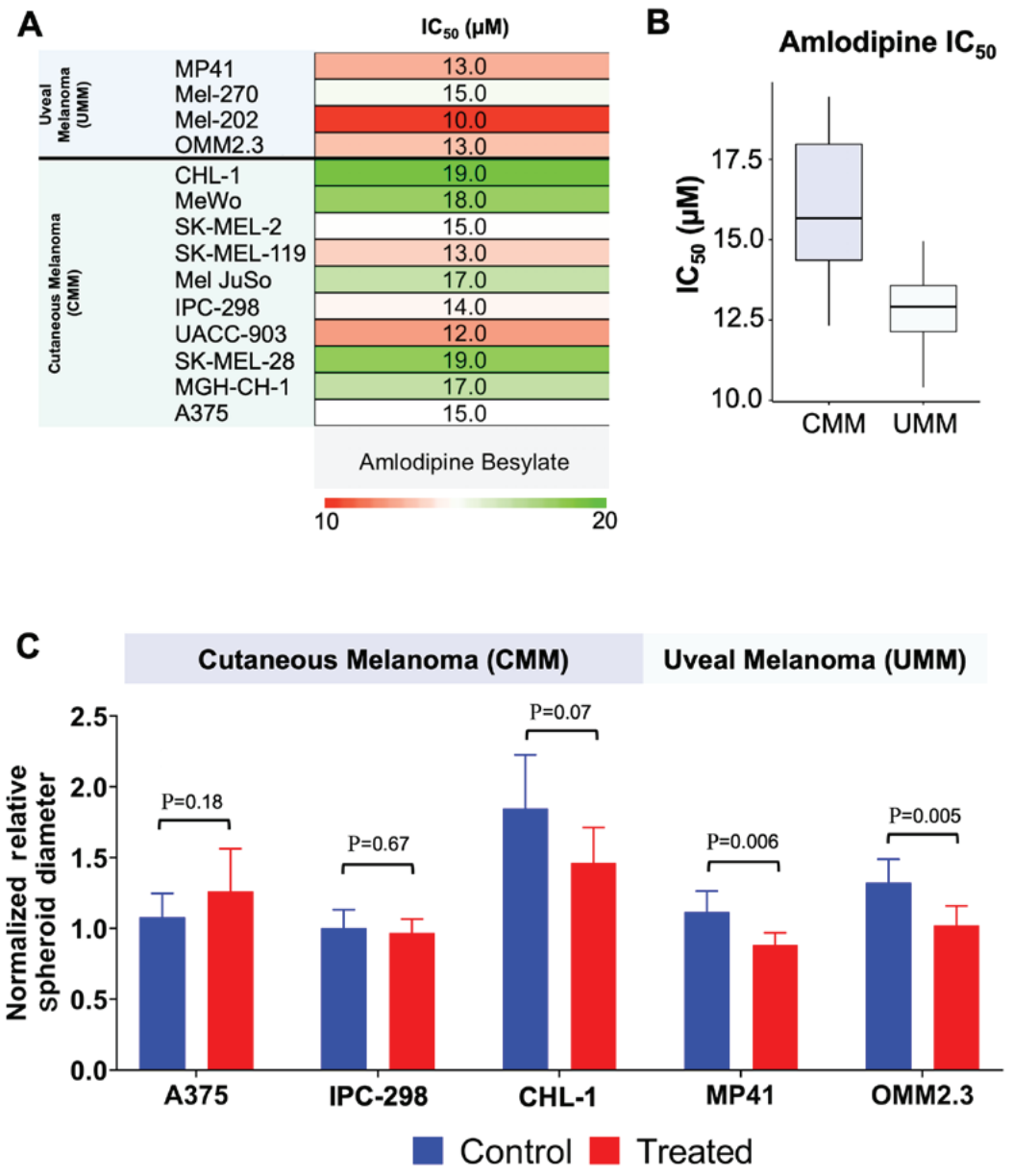

Figure 2. Amlodipine selectively inhibits UMM growth in 2D and 3D culture. (A) Heatmap of mean half maximal inhibitory [IC_{50} in (μM)] concentrations yielded by 2D drug screening on 10 CMM and 4 UMM cell lines. (B) Comparison of mean IC_{50} values in our cohort of CMM and UMM lines. (C) Summarized bar graph shows amlodipine selectively reduces diameters of UMM vs CMM spheroids after 48 h of treatment. P-values are from two-sided t-tests. UMM, uveal malignant melanoma; CMM, cutaneous malignant melanoma.

(P=0.0003, Mann-Whitney U test; Fig. 1B). During 2D screening in our cohort, amlodipine yielded an IC_{50} value of 12.8 μM in the UMM lines compared to 15.9 μM in the CMM lines (P=0.035; Figs. 2A and B). Treatment with both the non-dihydropyridine CCBs, verapamil and diltiazem, failed to reach 50% growth inhibition in either CMM or UMM (maximum concentration: 30 μM; data not shown). Rhod-2 staining demonstrated effective intracellular calcium depletion following 48 h of treatment with 1, 3 and 8 μM amlodipine in UMM. Contrarily, intracellular calcium levels were unaffected by amlodipine treatment in CMM (Fig. S1). Based on these preliminary results, we focused primarily on amlodipine rather than verapamil or diltiazem in all subsequent assays.

Spheroids subjected to 48 h of treatment with 20 μM amlodipine displayed, on average, a significantly decreased spheroid volume growth in UMM lines compared to the DMSO control. In the UMM line, MP41, control spheroid diameter increased by 11.5%, while the amlodipine-treated MP41 spheroids exhibited a decay of 11.6% (P=0.006). The OMM2.3 spheroids grew by 32.4%, while the amlodipine-treated spheroids grew an average of only 2.2% (P=0.005). In 3 separate colonies of CMM spheroids (A375, CHL-1 and IPC-298), there was no evidence of significant growth inhibition with amlodipine treatment compared to the DMSO control, and, in fact, the treated A375 spheroids appeared to grow more rapidly than their control counterparts (Figs. 2C and S2).

The UMM line, OMM2.3, exhibited an 87% induction of the early apoptotic marker, Annexin V, with 20 μM amlodipine treatment compared to 10% Annexin V induction with DMSO (P<0.0001). The induction was less pronounced at 21 and 31% by treatment with amlodipine at 5 and 10 μM (P=0.004 and P<0.0001, respectively). The MP41 cells exhibited a

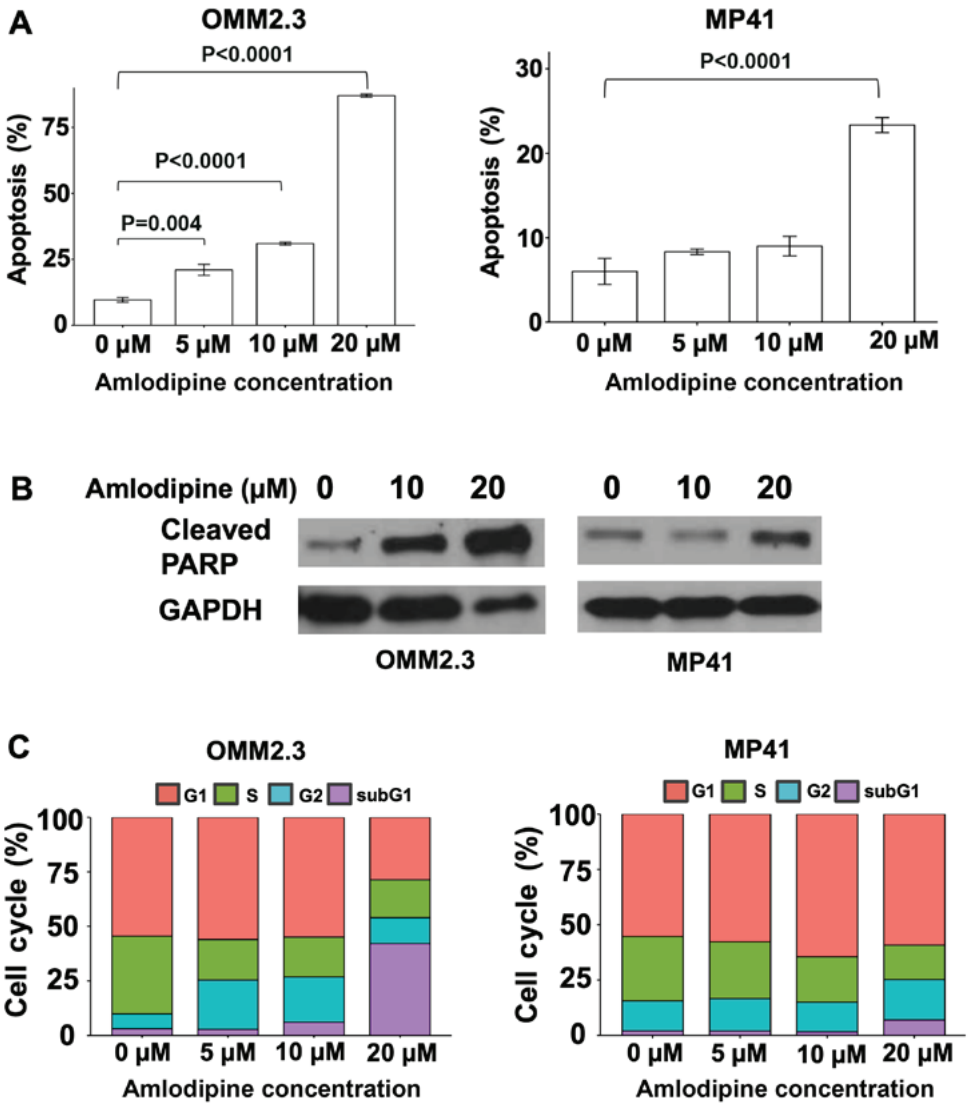

Figure 3. Amlodipine treatment induces apoptosis and cell cycle arrest. (A) Proportions of MP41 and OMM2.3 cells undergoing apoptosis (Annexin V$^+$) following treatment with amlodipine for 24 h. P-values are from one-way ANOVA and Dunnett's post hoc test for multiple comparisons. (B) Cleaved PARP expression measured by western blot analysis following treatment with various concentrations of amlodipine. (C) Cell cycle analyses with FACS showing G1 and G2 phase arrest and an increase in the sub-G1 cell population following treatment with amlodipine.

23% Annexin V induction with 20 μM amlodipine and 6% with DMSO (P<0.0001) (Fig. 3A). The amount of induction with lower concentrations of amlodipine did not differ significantly from the DMSO control. Western blot analysis of the MP41 and OMM2.3 cells for cleaved PARP, a known indicator of apoptosis, revealed that amlodipine treatment increased the levels of cleaved PARP in both lines in a dose-dependent manner (Fig. 3B). The observed effect was more prominent in the OMM2.3 cells. Cell cycle analysis demonstrated G1 and G2 phase arrest, S phase reduction and an increase in the number of cells in the sub-G1 phase in both the MP41 and OMM2.3 lines treated with amlodipine compared to the DMSO control (Fig. 3C). SA-β-gal did not reveal any marked changes in the presence or absence of amlodipine in CMM and UMM lines (Fig. S3).

Discussion

Considering the results of our unbiased library screening on the UMM line, OMM2.3, which was further confirmed in 2D and 3D experiments on larger cohorts, we hypothesized that the calcium signaling pathway may be a potentially useful therapeutic target in UMM. We demonstrated that amlodipine, which was represented twice amongst the top 10 active compounds of our candidate screening, significantly and selectively inhibited UMM growth when compared to that of CMM in both 2D and 3D culture systems. Furthermore, the spheroid growth inhibition observed in this study suggests that amlodipine can act biologically as a UMM-selective agent in a 3D tumor. We consider that amlodipine likely causes growth inhibition by mediating an increase in apoptosis and cell cycle arrest in UMM. We observed a consistent increase in apoptosis independently through both Annexin V and PARP assays, which further strengthens this finding. In addition, given our preliminary results, we consider that senescence is unlikely to markedly contribute to growth inhibition in UMM.

While our results support the role of calcium signaling in the proliferation and survival of UMM, the mechanism behind this association has not yet been defined. The

calcium signaling pathway, and its dysregulation, has a well-documented association with cancer survival, proliferation, migration and metastatic potential (13-16). For example, calcium signaling has been reported to be involved in the proliferation of *RAS*-driven cancers through the interaction of calmodulin (CaM) and PI3K (17) and the promotion of invasion and metastasis via ERK activation in both *BRAF*-driven and non-*BRAF* melanoma cells (18,19). One such example that could explain the selectivity we observed in UMM is RasGRP3, which was identified by Chen *et al* (2017) as a link between MAPK activation and the *GNAQ/11* mutations that characteristically drive UMM (20). *RasGRP3*, which is overexpressed in response to *GNAQ/11* mutations, reportedly drives the MAPK pathway through the activation of HRAS (20). RasGRP3 itself is activated both through phosphorylation by protein kinase C (PKC), which is calcium-activated, or through membrane recruitment by diacylglycerol kinase (DAG) (21), which similarly to RasGRP3 contains a calcium-binding EF-hand motif. The ability of calcium to potentially alter this unique UMM pathway, although speculative, is evidence of the multitude of possible avenues for the involvement of calcium signaling, and thereby calcium channel blockade, in the oncogenic landscape of UMM.

It is of particular interest that non-dihydropyridine CCBs demonstrated minimal to no inhibition in our UMM or CMM cell lines, which further suggests the involvement of a distinct and targetable alteration in the calcium signaling pathway in melanoma. Both families of CCBs are known to bind L-type calcium channels, but at different binding sites within the α1-subunit (22). It has been suggested that specific isoforms of the L-type channel are particularly upregulated in melanoma, while others are widely expressed in both melanoma and normal melanocytes (23), and each individual isoform has a particular pattern of tissue expression (24). Therefore, it is possible that the selectivity reported here is driven by a unique disparity of L-type calcium channel expression in UMM and CMM.

We recognize several limitations in our study. Our results stem from *in vitro* experiments and would likely benefit from further confirmatory work using animal models or human studies. Future research may also benefit from large-scale population studies of patients on long-term therapy with amlodipine and their risk for UMM, although this will remain challenging given the considerably low incidence of UMM. We also acknowledge that the variability in growth kinetics between UMM and CMM cell lines may partially explain the observed differences in cell viability and growth inhibition. We have partially addressed this limitation by controlling our drug treatments with DMSO solvent. It is possible that calcium plays a role in metabolic regulation over oncogenic activation, and the significance of other pathways cannot be excluded at this time. We recognize that the concentration of amlodipine used in our experiments is higher than what is typically achieved with standard dose for cardiovascular disease management, but we found that it is comparable to the micromolar range concentrations used in the literature to study amlodipine's antiproliferative effects on various cancers and other cell types (25-27). Finally, any mechanistic explanation discussed herein is only speculative, and studies that aim to further delineate the mechanism of action that validates our demonstrated inhibitory effects of amlodipine on UMM are currently underway.

In conclusion, UMM is an aggressive primary ocular tumor with a high risk of metastasis and no known effective treatments. We propose that calcium inhibition is one potential strategy for targeting UMM, as it has already demonstrated selective and significant *in vitro* growth inhibition in UMM compared to CMM. Based on the information gathered in this study, further preclinical trials in animal models and genetic studies utilizing gene silencing techniques of candidate genes are required to firmly establish calcium channel blockade as an effective therapeutic strategy as well as uncovering a possible mechanism of action.

Acknowledgements

Not applicable.

Funding

This study was supported in part by the US NIH (K24 CA149202 to HT) and by generous donors to Massachusetts General Hospital on behalf of melanoma research.

Availability of data and materials

All data generated or analyzed during this study are included in this published article or are available from the corresponding author on reasonable request.

Authors' contributions

MS, GLM, NK, ZJ, AR, RK, KF and HT were involved in the experimental design and conception of the study. MS, GLM, NK, ZH, AR and RK were involved in data acquisition. MS, GLM, NK, ZH, AR, RK, KF and HT were involved in data analysis and interpretation. MS, GLM, NK, ZH, AR, RK, KF and HT were involved in the preparation of the manuscript. All authors have read and approved the final manuscript.

Ethics approval and consent to participate

Not applicable.

Patient consent for publication

Not applicable.

Competing interests

The authors declare that they have no competing interests.

References

1. Shields CL, Furuta M, Thangappan A, Nagori S, Mashayekhi A, Lally DR, Kelly CC, Rudich DS, Nagori AV, Wakade OA, *et al*: Metastasis of uveal melanoma millimeter-by-millimeter in 8033 consecutive eyes. Arch Ophthalmol 127: 989-998, 2009.
2. Chattopadhyay C, Kim DW, Gombos DS, Oba J, Qin Y, Williams MD, Esmaeli B, Grimm EA, Wargo JA, Woodman SE, *et al*: Uveal melanoma: From diagnosis to treatment and the science in between. Cancer 122: 2299-2312, 2016.

3. Shaughnessy M, Klebanov N and Tsao H. Clinical and therapeutic implications of melanoma genomics. J Transl Genet Genom 2: 14, 2018:
4. Singh AD and Topham A: Incidence of uveal melanoma in the United States: 1973-1997. Ophthalmology 110: 956-961, 2003.
5. Kaliki S and Shields CL: Uveal melanoma: Relatively rare but deadly cancer. Eye (Lond) 31: 241-257, 2017.
6. Grisanti S and Tura A: Uveal melanoma. In: Noncutaneous melanoma. Scott JF and Gerstenblith MR (eds). Codon Publications, Brisbane, 2018.
7. Eskelin S, Pyrhönen S, Hahka-Kemppinen M, Tuomaala S and Kivelä T: A prognostic model and staging for metastatic uveal melanoma. Cancer 97: 465-475, 2003.
8. Field MG, Durante MA, Anbunathan H, Cai LZ, Decatur CL, Bowcock AM, Kurtenbach S and Harbour JW: Punctuated evolution of canonical genomic aberrations in uveal melanoma. Nat Commun 9: 116, 2018.
9. Augsburger JJ, Corrêa ZM and Shaikh AH: Effectiveness of treatments for metastatic uveal melanoma. Am J Ophthalmol 148: 119-127, 2009.
10. Desjardins L, Levy C, Lumbroso Le Rouic L, Cassoux N, Piperno-Neumann S, Mariani P, Servois V, Dendale R, Plancher C and Asselain B: Adjuvant intravenous therapy by fotemustine in uveal melanoma: A randomised study. Acta Ophthalmologica: Sep 15, 2011 (Epub ahead of print). doi. org/10.1111/j.1755-3768.2011.4362.x.
11. Komatsubara KM and Carvajal RD: Immunotherapy for the treatment of uveal melanoma: Current status and emerging therapies. Curr Oncol Rep 19: 45, 2017.
12. Jovanovic P, Mihajlovic M, Djordjevic-Jocic J, Vlajkovic S, Cekic S and Stefanovic V: Ocular melanoma: An overview of the current status. Int J Clin Exp Pathol 6: 1230-1244, 2013.
13. Stewart TA, Yapa KT and Monteith GR: Altered calcium signaling in cancer cells. Biochim Biophys Acta 1848: 2502-2511, 2015.
14. Brzozowski JS and Skelding KA: The multi-functional calcium/calmodulin stimulated protein kinase (CaMK) family: Emerging targets for anti-cancer therapeutic intervention. Pharmaceuticals (Basel) 12: 12, 2019.
15. Cui C, Merritt R, Fu L and Pan Z: Targeting calcium signaling in cancer therapy. Acta Pharm Sin B 7: 3-17, 2017.
16. Wang X, Liu H, Xu Y, Xie J, Zhu D, Amos CI, Fang S, Lee JE, Li X, Nan H, *et al*: Genetic variants in the calcium signaling pathway genes are associated with cutaneous melanoma-specific survival. Carcinogenesis 40: 279-288, 2019.
17. Nussinov R, Wang G, Tsai CJ, Jang H, Lu S, Banerjee A, Zhang J and Gaponenko V: Calmodulin and PI3K signaling in KRAS cancers. Trends Cancer 3: 214-224, 2017.
18. Maiques O, Barceló C, Panosa A, Pijuan J, Orgaz JL, Rodriguez-Hernandez I, Matas-Nadal C, Tell G, Vilella R, Fabra A, *et al*: T-type calcium channels drive migration/invasion in BRAFV600E melanoma cells through Snail1. Pigment Cell Melanoma Res 31: 484-495, 2018.
19. Umemura M, Baljinnyam E, Feske S, De Lorenzo MS, Xie LH, Feng X, Oda K, Makino A, Fujita T, Yokoyama U, *et al*: Store-operated Ca^{2+} entry (SOCE) regulates melanoma proliferation and cell migration. PLoS One 9: e89292, 2014.
20. Chen X, Wu Q, Depeille P, Chen P, Thornton S, Kalirai H, Coupland SE, Roose JP and Bastian BC: RasGRP3 mediates MAPK pathway activation in GNAQ mutant uveal melanoma. Cancer Cell 31: 685-696.e6, 2017.
21. Xie S, Naslavsky N and Caplan S: Diacylglycerol kinases in membrane trafficking. Cell Logist 5: e1078431-e1078431, 2015.
22. Opie LH. Pharmacological differences between calcium antagonists. Eur Heart J 18 (Suppl A): A71-A79, 1997.
23. Das A, Pushparaj C, Bahí N, Sorolla A, Herreros J, Pamplona R, Vilella R, Matias-Guiu X, Martí RM and Cantí C: Functional expression of voltage-gated calcium channels in human melanoma. Pigment Cell Melanoma Res 25: 200-212, 2012.
24. Striessnig J, Ortner NJ and Pinggera A: Pharmacology of L-type calcium channels: Novel drugs for old targets? Curr Mol Pharmacol 8: 110-122, 2015.
25. Zou J, Li Y, Fan HQ and Wang JG: Effects of dihydropyridine calcium channel blockers on oxidized low-density lipoprotein induced proliferation and oxidative stress of vascular smooth muscle cells. BMC Res Notes 5: 168, 2012.
26. Lee H, Kang S and Kim W: Drug repositioning for cancer therapy based on large-scale drug-induced transcriptional signatures. PLoS One 11: e0150460, 2016.
27. Ohba T, Watanabe H, Murakami M, Radovanovic M, Iino K, Ishida M, Tosa S, Ono K and Ito H: Amlodipine inhibits cell proliferation via PKD1-related pathway. Biochem Biophys Res Commun 369: 376-381, 2008.